CHARACTERIZATION OF CDK9 ROLE IN THE DNA DAMAGE RESPONSE

THALES DA COSTA NEPOMUCENO[1], GUILHERME SUAREZ-KURTZ[1], ALVARO NUNES DE ALMEIDA MONTEIRO[2], MARCELO ALEX DE CARVALHO[1,3]

[1] Instituto Nacional de Câncer – Divisão de pesquisa clínica

[2] Moffitt Cancer Center - Cancer Epidemiology Program

[3] Instituto Federal do Rio de Janeiro – Divisão de Biotecnologia.

INTRODUCTION

The DNA damage response (DDR) is a well-coordinated pathway capable of sensing and repairing different types of DNA damage. Double-strand break (DSB) lesions activate the ATM-CHK2 axis, which is responsible for the cell cycle arrest, prompting cells for DNA repair. DSBs are primarily repaired through two distinct pathways: homology-directed recombination (HR) and non-homologous end-joining (NHEJ). BRCA1 and 53BP1 play an important role in DDR by orchestrating the decision between HR and NHEJ, but the precise mechanisms regarding both pathways are not entirely understood. Previously, our group identified the putative interaction of the cyclin-dependent kinase 9 (CDK9) with BRCA1 and BARD1 (BRCA1-associated RING domain 1). CDK9 is a component of the positive transcription elongation complex and has been implicated in genome integrity maintenance associated with the replication stress response. More recently, we characterized CDK9 as a DDR player by modulating BRCA1 recruitment to DNA damaged sites and consequently the HR pathway.

METHODS AND RESULTS

Here we show that cells lacking CDK9 failure to form RAD51, but not 53BP1, ionizing radiation-induced foci (IRIF) and are characterized by an increased sensitivity to PARP inhibition in the presence DSBs. Our data suggest that the CDK9-BRCA1 interaction (through BRCA1 N-terminal region) is dependent on BRCA1-BARD1 heterodimer formation. We identified a CDK9 mutant (E369A) that abrogates the CDK9-BRCA1 interaction (through BRCA1 C-terminal region). Moreover, we characterized CHK2 as a novel CDK9-interaction partner, through ectopic GST-pulldown and constitutive co-immunoprecipitation assays. Cells lacking CDK9 are deficient in promoting G2/M arrest after IR-induced DNA damage. We also identified new CDK9 interactions in a DDR-related context using a TAP-MS approach.

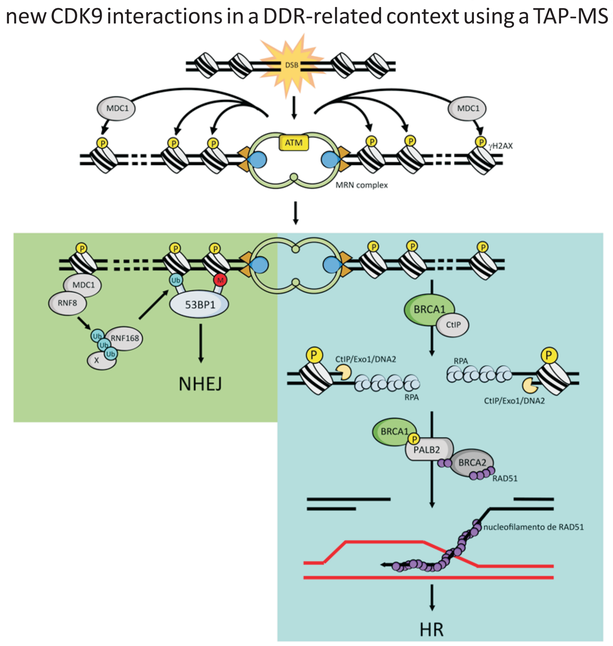

Figure 1. The DNA damage repair by homologous recombination and non-homologous end-joining.
Schematic representation of double strand break (DSB) resolution by homologous (HR; blue background) or non-homologous end-joining (NHEJ; green background) pathways. The MRN (MRE11-RAD50-NBS1) sensor complex recognizes and binds DSBs. ATM is then recruited and activated, leading to the phosphorylation of H2AX (γH2AX), amplifying the initial signaling. The signal transduction leads to BRCA1 or 53BP1 recruitment to the DNA damaged site, driving the HR or NHEJ repair, respectively.
53BP1 recruitment is mediated by nucleosome methylation and ubiquitylation, which promotes NHEJ. BRCA1 recruitment stimulates the DNA 5' end resection and subsequently the formation of the BRCA1-PALB2-BRCA2 complex. This complex recruit the recombinase RAD51, which is responsible for the sister chromatid strand invasion and error-free repair.

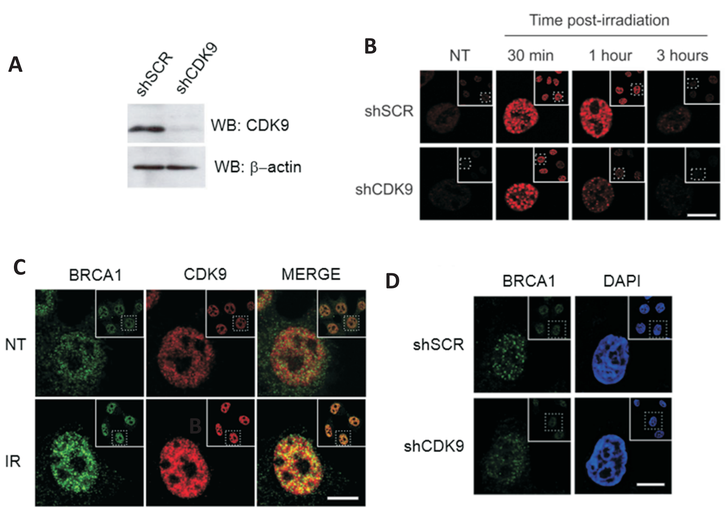

Figure 2. CDK9 is a DDR-related protein.
(**A**) CDK9 protein profile in MCF7 shSCR (negative control) and MCF7 shCDK9 nuclear extracts. TBP was used as loading control.
(**B**) γH2AX foci dynamics in CDK9-silenced cells. Cells were exposed to IR (5 Gy) and immunostained after the indicated time intervals using anti-phosphorylated H2AX (Ser139). Insets depict the nucleus in lower magnification. Scale bars = 10 μm
(C) CDK9 IRIF co-localize with BRCA1 at damaged DNA sites. MCF7 cells were exposed to IR (10 Gy) and recovered for 3 hours. Immunostaining was performed using anti-CDK9 and anti-BRCA1 antibodies. Insets depict the nucleus in lower magnification. NT, not treated. Scale bars = 10μm
(**D**) BRCA1 recruitment to DSB sites is dependent on CDK9. MCF7 shSCR and shCDK9 cells were exposed to IR (10 Gy) and recovered for 3 hours. Immunofluorescence staining using anti-BRCA1. Insets depict the nucleus in lower magnification. Scale bars = 10 μm

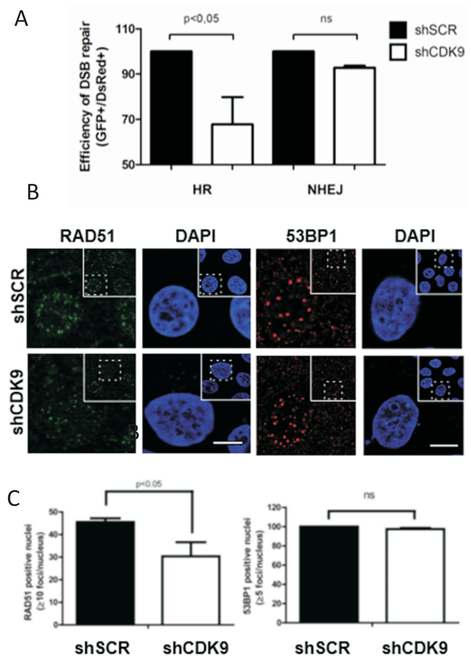

Figure 3. CDK9 plays a role on DNA damage repair by modulating the HR pathway.
(**A**) HR and NHEJ repair efficiency quantification in cells lacking CDK9 expression. Cells were analyzed 72 hours after co-transfection of linearized reporter plasmids (HR or NHEJ) and the DsRed expression vector. Data is presented as mean +/- SD of percentage of GFP positive cells relative to DsRed positive cells.
(**B**) The recruitment of RAD51, but not 53BP1, is mediated by CDK9. MCF7 shSCR or shCDK9 cells were exposed to IR (10 Gy) and recovered for 3 hours and 5 hour and stained using anti-53BP1 and anti-RAD51, respectively. Insets depict the nucleus in lower magnification. Scale bars = 10 μm.
(**C**)53BP1 and RAD51 foci quantification using Image J software. Data is presented as mean +/- SD.

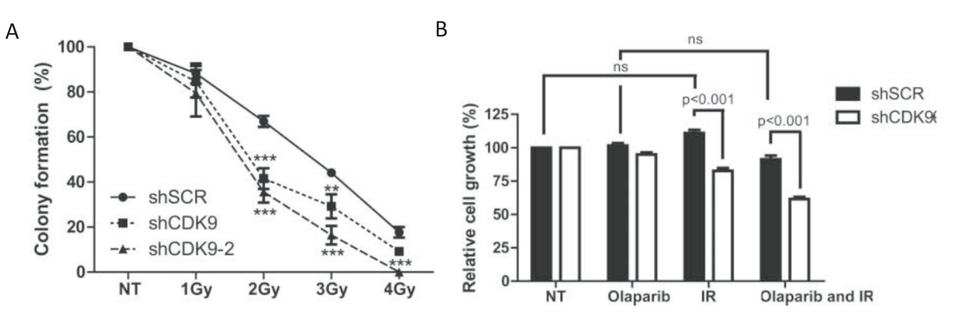

Figure 4. Cells lacking CDK9 exhibit increase sensitivity to genotoxic agents.
(**A**) MCF7 shSCR, shCDK9 and shCDK9–2 were subjected to long-term clonogenic assay after irradiation (1, 2, 3 or 4 Gy). Cells were fixed and stained with crystal violet and colonies were quantified. Data are presented as means +/- SD of triplicates. *** = $p<0.001$ and ** = $p<0.01$
(**B**) Cells were also subjected to viability assay after treatment with ionizing radiation in the presence or not of PARP inhibitor, olaparib (50 nM). Viability quantification were determined by the absorbance of crystal violet at 590 nm. Data are presented as means +/- SD of triplicates.

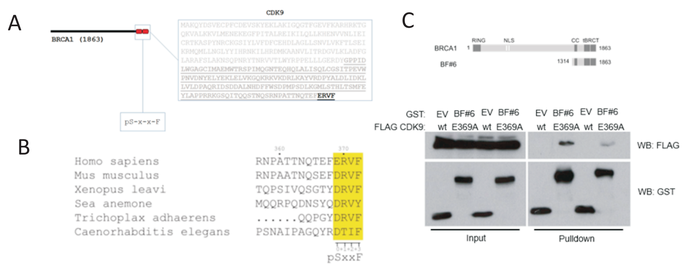

Figure 5. Structural characterization of the CDK9/BRCA1 interaction.
(**A**) Schematic representation of the CDK9 protein region identified for interacting with BRCA1 tBRCT (underlined sequence; Woods et al., 2012) and the consensus sequence of BRCA1 tBRCT domain phosphopeptide recognition.
(**B**) Orthologue align of CDK9 C-terminal region. Conserved region that mimics the BRCA1 tBRCT phosphopeptide recognition sequence is highlighted in yellow.
(C) (**Upper panel**) Schematic diagram representing the BRCA1 construct used in the pulldown assay (BF#6). (**Lower panel**) Co-expression (input) and pulldown of GST-fragment of BRCA1 (BF#6) or control (empty vector; EV) and FLAG-CDK9 wild-type (wt) or E369A mutated in HEK293FT cells. Western blots (WB) were developed using indicated antibodies.

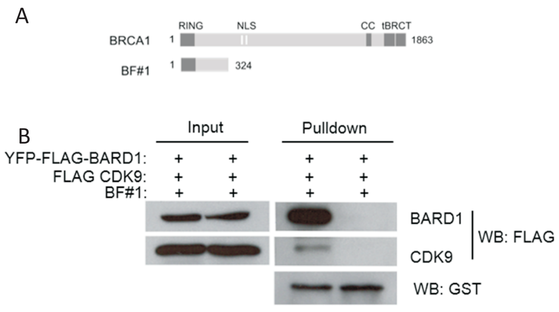

Figure 6. Structural characterization of the CDK9/BRCA1/BARD1 interaction.
(**A**) Schematic diagram of the BRCA1 construct used in the pulldown assay (BF#1).
(**B**) Co-expression (input) and pulldown of GST-fragment of BRCA1 (BF#1), FLAG-CDK9 and YFP-FLAG-BARD1 in HEK293FT cells. Western blots (WB) were developed using indicated antibodies.

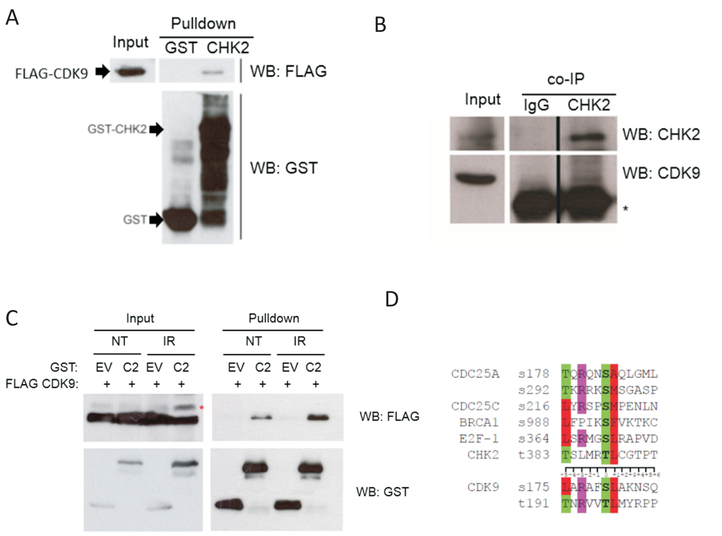

Figure 7. Characterization of the CDK9/CHK2 interaction.
(**A**) GST-CHK2 expressed in bacterial cells and FLAG-CDK9 produced in HEK293FT (input) for GST-pulldown. WBs were developed using indicated antibodies. The arrows indicate the respective protein product.
(**B**) Protein levels were determined in MCF7 extracts by immunoblotting using specific antibodies. Co-immunoprecipitation assays were performed using anti-CHK2 or anti-FLAG (IgG) antibodies, immunoblots were developed using anti-CDK9 and anti-CHK2 antibodies, as indicated. * indicates the IgG light chain.
(C) Co-expression (input) and pulldown of GST-tagged CHK2 (C2) or control (empty vector; EV) and FLAG-CDK9 in HEK293FT cells. Western blots (WB) were developed using indicated antibodies. The asterisk indicates a putative phosphorylation of FLAG-tagged CDK9.
(**D**) Homology line-up of CHK2 substrates and two putative phosphorylation sites in CDK9 primary amino acid sequence. Phospho-acceptor serine or threonine are highlighted in bold. Amino acids are grouped in five categories: the ones with small lateral chains (Red), with basic lateral chains (Pink), with hydroxyl, sulfhydryl or amine groups in the lateral chain (Green) and the others (colorless).

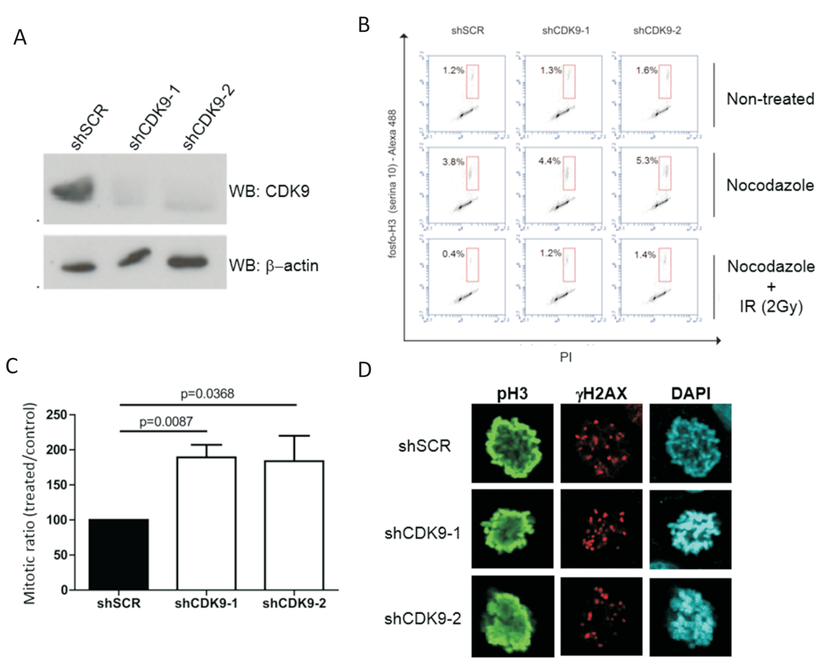

Figure 8. CDK9 modulates the G2/M transition after DNA damage.
(**A**) CDK9 protein profile in MCF7 shSCR (negative control) MCF7 shCDK9-1 and MCF7 shCDK9-2 extracts. β-actin was used as loading control.
(**B**) MCF7 shSCR, shCDK9-1 and shCDK9-2 cells were exposed to 2 Gy of ionizaing radiation in the presence or absence of nocodazole. Cells were harvested 4 hours after IR treatment and analyzed by flow cytometry using anti-phosphoH3 (serine 10; pH3) and propidium iodide. © Quantification is presented as mean +/- SD of the normalized ratio between treated and control pH3 positive cells.
(**D**) Immunofluorescence analysis using anti-pH3 and anti-gH2AX of MCF7 shSCR, shCDK9-1 and shCDK9-2 cells, following the same treatment presented in C.

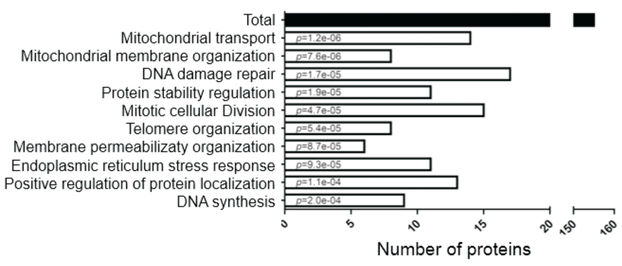

Figure 9. Gene onthology profile of CDK9 interacting proteins in a DDR context.
HEK293FT overexpressing pNTAP-CDK9 were exposed to IR (10 Gy) and recovered for 3 hours. The interactome was obtained after tandem affinity purification, by mass spectrometry. The gene onthology (GO) enrichment was obtained by the WebGestalt softwere.

CONCLUSION

Collectively, our data suggest a role for CDK9 in the DDR through DNA damage repair and cell cycle checkpoint regulation.

Projeto Gráfico: Setor de Edição e Informação Técnico-Científica / INCA

MINISTÉRIO DA SAÚDE